Estimate of the melanin content in human hairs by the inverse Monte-Carlo method using a system for digital image analysis

A.N. Bashkatov, E.A. Genina, V.I. Kochubei, V.V. Tuchin

Abstract. **Based on the digital image analysis and inverse Monte-Carlo method, the proximate analysis method is developed and the optical properties of hairs of different types are estimated in three spectral ranges corresponding to three colour components. The scattering and absorption properties of hairs are separated for the first time by using the inverse Monte-Carlo method. The content of different types of melanin in hairs is estimated from the absorption coefficient. It is shown that the dominating type of melanin in dark hairs is eumelanin, whereas in light hairs pheomelanin dominates.**

Keywords: *absorption, scattering, colour analysis, inverse Monte-Carlo method, melanin.*

1. Introduction

The knowledge of optical parameters of biological tissues is a key factor in the development of theoretical models describing the propagation of light in biological tissues (in particular, human hairs). These models can be used for solving many important problems in laser therapy, diagnostics of various diseases, the interpretation of spectrophotometric measurements, etc. However, despite the growth of the number of papers devoted to the measurements of optical parameters of biological tissues or development of methods for measuring these parameters, the optical parameters of many biological tissues, their morphological properties and component composition still remain inadequately studied [1 – 3].

Analysis of the melanin content in various biological tissues occupies a prominent place in modern biomedical optics. This problem attracts interest first of all in dermatology and cosmetology, where the development of new and more efficient methods of diagnostics and medical treatment of various skin and hair diseases, laser hair removal, etc. requires a knowledge of the concentration and physico-chemical properties of this pigment [4 – 6]. The content of melanin in human hairs was studied in many papers [7 – 19]. The melanin concentration was measured by the methods of

A.N. Bashkatov, E.A. Genina, V.I. Kochubei, V.V. Tuchin Department of Optics and Biomedical Physics, N.G. Chernyshevskii Saratov State University, ul. Astrakhanskaya 83, 410012 Saratov, Russia;
e-mail: bash@optics.sgu.ru

liquid chromatography [8, 10, 12, 16, 19] and microspectro-photometric analysis in a broad wavelength range [7, 9, 18, 19]. Low-coherence reflectometry is also a promising method, which can be used for measurements along and across a hair with a high spatial resolution [11]. However, these measuring systems and methods are quite expensive, laborious, and require a long time (of the order of a few tens of hours) for analysis. Therefore, the development of new efficient and low-cost methods of proximate analysis of the melanin content in biological tissues is of current interest.

The method of digital image analysis is promising for estimates of the melanin content in tissues. Systems for digital image analysis are now widely used in dermatology to study small skin areas during skin diseases, to analyse a colour background, and obtain colour information at each point forming an image [6, 20 – 31]. We performed earlier preliminary studies of hairs based on the digital image analysis [13 – 15] with the aim to develop a system for the proximate analysis of optical parameters of hairs and estimates of the melanin content in them. However, these studies were only preliminary and require a further development taking into account the morphological and optical (especially scattering) properties of hairs.

The aim of this paper is the development of the method for proximate analysis of the optical parameters of hairs and estimates of the melanin content in hairs of different types.

2. Structure and composition of hairs

A human hair has the form of a truncated cone of diameter from 10 to 250 μm. The external shell of the hair (cuticle) is formed by a thin (approximately 10 % of the hair weight) but rigid enough carcass consisting mainly of keratin and proteolipids forming the hydrophobic membrane of the hair [32, 33]. The internal part of the hair (cortex) is formed by keratinised fibres surrounded by a sulphur-containing matrix and three specialised types of cells responsible for metabolism and morphology of the hair [32]. The hair cortex also contains melanin granules and accounts for about 90 % of the hair weight [33]. The colour of human hairs is determined by their structure and the concentration and type of melanin contained in them: eumelanin, which is mainly black and turns hairs to black and chestnut colours, and yellow or reddish pheomelanin, which turns hairs to lighter tints [7 – 9, 16 – 19, 33].

It was shown in [16] that eumelanin dominates in hairs of all types. Thus, black hairs contain 99 % of eumelanin and 1 % of pheomelanin, chestnut and blond hairs contain 95 % of eumelanin and 5 % of pheomelanin, and only red

Table 1. Melanin concentration in hairs of different types reported in the literature.

Hair colour	Melanin concentration / mg g^{-1}				
	[12]	[10]	[17]	[18]	[16]
Black	13.485	–	5.37	31 ± 15 [1]	7.2
White (blond)	3.46 ± 0.73 [2]	–	1.165	–	2.5
White (albino)	0.65	–	1.626	–	–
Red (different tints)	39.85 ± 52.48 [3]	4.065	1.9 ± 0.7 [2]	–	2.5
Dark chestnut	10.175	3.3 ± 1.5 [4]	3.2	–	5.2
Chestnut	5.55	2.64 ± 0.92 [5]	3.086	–	–
Light chestnut	–	2.065	1.605	–	–
Light brown	–	2.23	1.281	–	–

[1] Averaged over three values; [2] averaged over two values; [3] averaged over ten values; [4] averaged over six values; [5] averaged over four values.

hairs contain 67 % of eumelanin and 33 % of pheomelanin. However, it follows from [19] that eumelanin and pheomelanin are contained in hairs of different types in approximately the same proportion. At the same time, the authors of papers [8–10, 12, 17] showed that pheomelanin dominates in light hairs, while eumelanin dominated in dark hairs.

Data on the melanin concentration in hairs of different types are also rather contradictory (Table 1). One can see from Table 1 that the melanin concentration in black hairs varies, according to the data reported by different authors, from 31 to 5.37 mg g^{-1} (concentration is expressed in milligrams of melanin in 1 g of hair), i.e. changes approximately by a factor of six. Even greater variation is observed for red hairs of different tints. The three-fold spread in the melanin concentration takes place even in hairs of albinos. It seems that such a great spread is caused by the complexity of systematisation of the hair colour, which is subjective to a great extent, and by the use of different methods for melanin separation. Thus, for example, it was shown in [18] that the mass concentration of melanin separated from hairs of the same type by different methods was 2.2 %, 4.8 %, and 2.3 %.

The scattering properties of a hair are determined by its inhomogeneous structure. A white colour of hairs observed in the absence of melanin is caused by an optical effect appearing due to refraction and reflection of beams inside the hair, which are incident on interfaces with different refractive indices.

Therefore, non-pigmented hairs with a great amount of a cerebral substance (cortex) are, as a rule, lighter than hairs without cortex. The same effect is observed for worn and brittle hairs – cortex and cuticle become discontinuous and form numerous interfaces with internal reflection and refraction of light [34]. Newly formed non-pigmented hairs, devoid of cortex, are yellowish rather than white, which is probably related to the presence of dense keratin [34].

Hairs turn grey, as a rule, due to aging, which is explained by a gradual weakening of the functioning of melanocytes and the formation of air regions inside a hair. In greying hairs the pigment is gradually destroyed, i.e. a full spectrum of colours, beginning from natural (for a given person) to white, can be observed along the length of a hair and from hair to hair. The amount of melanocytes in grey hairs is very low or they are absent at all or can be in the inactive state [34].

Thus, the absorption of light in hairs is determined by absorption in melanin contained in them, while scattering of light in hairs occurs from keratin scales of the hair cuticle and melanin granules located in cortex. Scattering of light in hairs of adults also occurs from air bubbles inside hairs formed due to the destruction of melanin granules.

3. Materials and methods

Hair samples for studies were taken from 10 volunteers. The first series of hair samples was obtained from a 19 years old brown-haired girl, the second one – from a 20 years old brunette girl, the third one – from a 45 years old light brown-grey-haired man, the fourth one – from a 19 years old blond girl, the fifth one – from a 60 years old grey-haired woman (light brown-haired in youth), the sixth one – from a 70 years old grey-haired woman (brown-haired in youth), the seventh and eighth ones – from 20 years old dark light brown-haired girls, the ninth one – from a 70 years old grey-haired man (light brown-haired in youth), and the tenth one – from a 35 years old dark light brown-haired man. Each of the series contained 30 hair samples.

The hair reflection and transmission coefficients were measured *in vitro* by using the experimental setup (Fig. 1) with the digital analysis of hair images. The hair reflection and transmission coefficients could be measured within certain spectral regions corresponding to the basic colours in the RGB colour coordinate systems: red, green, and blue. In [13], the wavelengths of maxima and half-width of spectral bands corresponding to the three used colour components were estimated: red ($\lambda_R = 600$ nm, $\Delta\lambda_R = 51.4$ nm), green ($\lambda_G = 540$ nm, $\Delta\lambda_G = 74.1$ nm), and blue ($\lambda_B = 460$ nm, $\Delta\lambda_B = 47$ nm).

A colour analysis system includes a colour video camera (SVHS Sony, CCD-TR617E PAL, Japan) combined with a microscope, which gives the colour image of a sample and
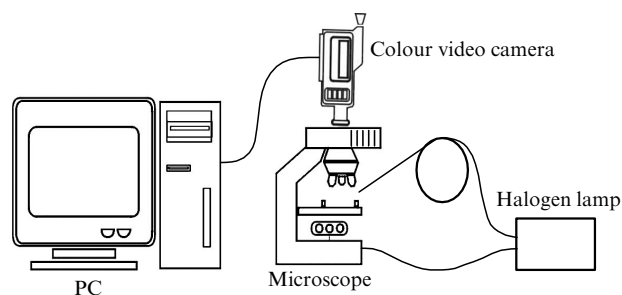
Figure 1. Scheme of the experimental setup.

transfers the data to a PC for processing, and a sample fixed on a special plate. Depending on the hair imaging conditions (in transmitted or reflected light), this plate was either a transparent microscope slide or a black-and-white test object with a hair fixed on it, which was used to provide identical imaging conditions during video camera self-tuning, in particular, to minimise the gamma correction of images. Test objects were dense black and white paper samples glued on a plate. Samples were illuminated through an optical fibre coupled with a halogen lamp.
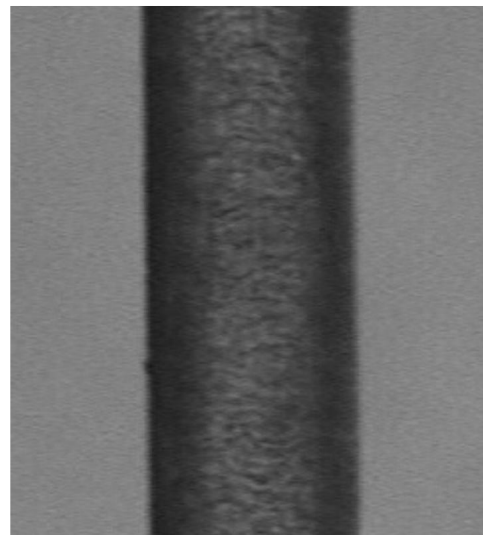
If an object (human hair) was imaged in transmitted light, the light was delivered through an optical fibre under the microscope stage perpendicular to the object. The object was illuminated through a ground glass to provide the uniform illumination of the video-camera field of view. Radiation from a halogen lamp transmitted through the ground glass was focused with a lens to the object. When the image of an object was recorded in reflected light, light from the halogen lamp was delivered to the object from above at an angle of $\sim 45°$ between the plane in which the object was located (the microscope stage) and the normal to its surface. Such an experimental geometry eliminates flashes, provides the uniform illumination of the entire object, and prevents the incidence of the specular Fresnel reflection component on the video camera objective. The size of the illuminated region (10 mm $\times$ 10 mm) exceeded the field of view of the system (1 mm $\times$ 1 mm), providing the uniform illumination of the object. We used a $20^\times$ microscope objective with the numerical aperture of 0.4. The diameter of each hair was measured with a micrometer before experiments. In addition, the hair thickness was estimated during image processing by the method [14, 15] in which the image of a cylindrical object of the known diameter was recorded and its diameter was calculated in pixels, which provided the measurement of the hair diameter with an accuracy to a few fractions of micron.

The hair image was transferred as a standard BMP file to a PC for processing. The image was represented as a set of data with a spatial resolution of 720 (along horizontal) $\times$ 540 (along vertical) pixels and a colour resolution of 256 colour gradations for each of the colour components. Typical images of a light-brown hair obtained in reflected and transmitted light are presented in Figs 2 and 3.

The images of a hair fixed on a special plate were decomposed into three colour components by using the


Figure 3. Typical photograph of a light brown hair obtained in transmitted light with the $200^\times$ magnification.

Mathcad 2001 Professional Software (MathSoft, Inc., USA) with the in-built set of standard functions for image processing. The hair image for each of the colour components was scanned over its cross section by using a slit of width 21 pixels. The scan region was chosen visually to avoid flashes, illuminations, images of dust particles, etc, on the hair image. The brightness of individual pixels was averaged within the scan band. Figures 4 and 5 present typical curves illustrating this operation.
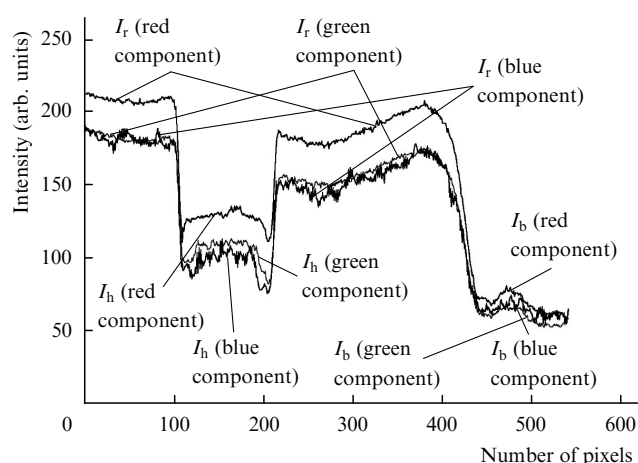
Figure 4. Intensity distributions in the cross section of the image of a light brown hair fixed on a special plate obtained in reflected light for three colour components (I_r is the image brightness for a white test object).

The reflection coefficient R of a hair was measured as the ratio of the hair image brightness I_h to the brightness I_r of the image of a white test object on which the hair was fixed. In addition, the background illumination of the image by external radiation sources was compensated by subtracting the brightness I_b of the black test object both from the hair brightness and the brightness of the white test object. As a result, the expression for the reflection coefficient R has the form

Figure 2. Typical photograph of a light brown hair obtained in reflected light with the $200^\times$ magnification.
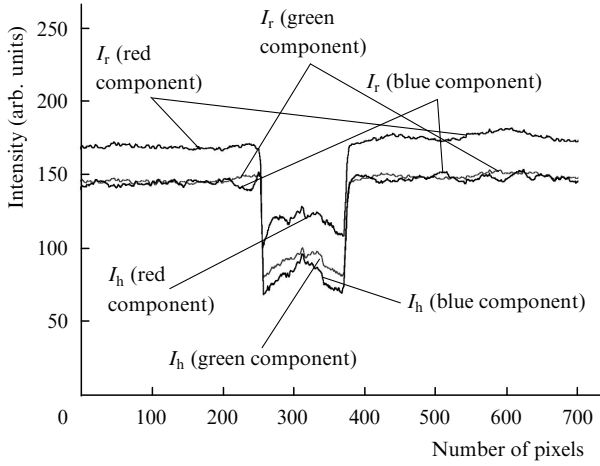
Figure 5. Intensity distributions in the cross section of the image of a light brown hair fixed on a special plate obtained in transmitted light for three colour components (I_r is the image brightness for a transparent microscope slide).

$$R = \frac{I_h - I_b}{I_r - I_b}. \qquad (1)$$

The hair transmission coefficient T was defined as the ratio of the hair-image brightness I_h to the image brightness I_r of the transparent microscope slide:

$$T = \frac{I_h}{I_r}. \qquad (2)$$

Because, as follows from Figs 4 and 5, the brightness distribution in the hair scan region in the direction from the hair centre to its periphery changes considerably, which is explained by the hair structure, i.e. by the dependence of the hair thickness on the radial coordinate, the values of I_h, I_r, and I_b obtained during scanning of the corresponding image regions were averaged.

The hair absorption and scattering coefficients were determined from the measured reflection and transmission coefficients by using the inverse Monte-Carlo method, which is widely used in the optical studies of biological tissues because it allows one to take into account the structure of a biological tissue, parameters of the experimental setup, the measurement geometry, the size and shape of the incident and detected beams, reflections at the interfaces of the medium layers, and other parameters [2, 35 – 37]. The direct problem was solved by using the statistical simulation algorithm described in detail in [37].

The Monte-Carlo method is based on the calculation of many random photon trajectories in a scattering medium, whose optical properties determine the length and shape of individual trajectories, and the subsequent statistical processing of the results obtained. The main input parameters of simulations are absorption (μ_a) and scattering (μ_s) coefficients of the medium, the scattering anisotropy factor g and the refractive index n. We assumed in our calculations here that the anisotropy factor was 0.8. The hair refractive index was fixed and equal to 1.5 [38]. We used 10^6 photon packets in Monte-Carlo simulations, each of them containing 10^4 photons. The photon trajectories in the medium were calculated by using the Henyey – Greenstein phase function

$$f_{HG} = \frac{1}{4\pi} \frac{1 - g^2}{(1 + g^2 - 2g\cos\theta)^{3/2}},$$

where θ is the polar scattering angle. The distribution over the azimuthal scattering angle was assumed homogeneous. A hair was simulated by an infinitely long uniform cylinder of specified diameter. It was assumed in simulations, based on the hair structure, that both absorbing and scattering centres are uniformly distributed over the entire volume of the hair follicle. Monte-Carlo simulations took into account the real illumination and detection geometry, i.e. the numerical aperture of the microscope.

The inverse problem of determining the coefficients μ_a and μ_s' of hairs was solved by minimising the goal function

$$F(\mu_a, \mu_s') = [R(\mu_a, \mu_s') - R^{exp}]^2 + [T(\mu_a, \mu_s') - T^{exp}]^2, \quad (3)$$

where $R(\mu_a, \mu_s')$, $T(\mu_a, \mu_s')$ and R^{exp}, T^{exp} are calculated and measured hair reflection and transmission coefficients, respectively, for each of the colour components. Iterations were performed by the simplex Nelder – Meed method described in detail in [39]. The initial values of μ_a and μ_s' were calculated from expressions [40]

$$\frac{\mu_s'}{\mu_a - \mu_s'} = \begin{cases} 1 - \left(\frac{1 - 4R - T}{1 - T}\right)^2 & \text{for} \quad \frac{R}{1 - T} < 0.1, \\ 1 - \frac{4}{9}\left(\frac{1 - 4R - T}{1 - T}\right)^2 & \text{for} \quad \frac{R}{1 - T} \geqslant 0.1, \end{cases}$$

$$(\mu_a + \mu_s')d = \begin{cases} -\frac{\ln T \ln 0.05}{\ln R} & \text{for} \quad R \leqslant 0.1, \\ 2^{1+5(R+T)} & \text{for} \quad R > 0.1, \end{cases}$$

where $\mu_s' = \mu_s(1 - g)$ is the transport scattering coefficient and d is the hair diameter. The condition

$$\frac{|R^{exp} - R^{calc}|}{R^{exp}} + \frac{|T^{exp} - T^{calc}|}{T^{exp}} < 0.01$$

was used as the criterion for the end of iterations, where R^{exp}, R^{calc} and T^{exp}, T^{calc} are the experimental and calculated hair reflection and transmission coefficients, respectively.

The hair absorption coefficients in the first approximation determined for spectral regions corresponding to the colour RGB components can be calculated from expressions

$$\mu_a^{460} = C_m[\varphi_{eu}\varepsilon_{eu}^{460} + (1 - \varphi_{eu})\varepsilon_{pheo}^{460}],$$

$$\mu_a^{540} = C_m[\varphi_{eu}\varepsilon_{eu}^{540} + (1 - \varphi_{eu})\varepsilon_{pheo}^{540}], \qquad (4)$$

$$\mu_a^{600} = C_m[\varphi_{eu}\varepsilon_{eu}^{600} + (1 - \varphi_{eu})\varepsilon_{pheo}^{600}],$$

where φ_{eu} is the eumelanin fraction in the hair (the pheomelanin fraction is $1 - \varphi_{eu}$); C_m is the total (eumelanin + pheomelanin) melanin concentration (in mg mL^{-1}); $\varepsilon_{eu}^{460} = 10.11$, $\varepsilon_{eu}^{540} = 6.25$ and $\varepsilon_{eu}^{600} = 4.3$ are the extinction coefficients of eumelanin (in mL cm^{-1} mg^{-1}); and $\varepsilon_{pheo}^{460} = 7.42$, $\varepsilon_{pheo}^{540} = 3.35$ and $\varepsilon_{pheo}^{600} = 1.74$ are the extinction coefficients

Table 2. Experimental data obtained by digital processing of hair images.

Series number	$d/\mu m$	Red component		Green component		Blue component	
		T	R	T	R	T	R
I	57.6 ± 7.2	0.69 ± 0.18	0.02 ± 0.01	0.62 ± 0.18	0.03 ± 0.01	0.47 ± 0.12	0.03 ± 0.02
II	57.7 ± 4.8	0.63 ± 0.14	0.01 ± 0.01	0.55 ± 0.11	0.02 ± 0.01	0.38 ± 0.05	0.03 ± 0.03
III	48.2 ± 4.0	0.52 ± 0.07	0.09 ± 0.03	0.47 ± 0.06	0.11 ± 0.05	0.39 ± 0.06	0.14 ± 0.07
IV	39.9 ± 5.0	0.58 ± 0.09	0.08 ± 0.02	0.55 ± 0.08	0.08 ± 0.02	0.48 ± 0.07	0.10 ± 0.04
V	48.7 ± 5.8	0.50 ± 0.06	0.11 ± 0.02	0.45 ± 0.05	0.10 ± 0.02	0.40 ± 0.05	0.12 ± 0.03
VI	36.9 ± 2.6	0.58 ± 0.08	0.08 ± 0.02	0.52 ± 0.07	0.10 ± 0.03	0.47 ± 0.07	0.10 ± 0.04
VII	49.9 ± 5.2	0.67 ± 0.03	0.05 ± 0.02	0.61 ± 0.05	0.05 ± 0.03	0.50 ± 0.03	0.10 ± 0.08
VIII	60.2 ± 5.1	0.56 ± 0.07	0.07 ± 0.02	0.50 ± 0.06	0.09 ± 0.06	0.38 ± 0.04	0.11 ± 0.06
IX	41.6 ± 4.3	0.47 ± 0.07	0.11 ± 0.03	0.43 ± 0.07	0.11 ± 0.03	0.37 ± 0.05	0.14 ± 0.05
X	49.2 ± 4.1	0.62 ± 0.03	0.07 ± 0.03	0.54 ± 0.02	0.08 ± 0.04	0.43 ± 0.02	0.12 ± 0.09

of pheomelanin at wavelengths 460, 540 and 600 nm, respectively [41]. The absorption of light in other hair components (for example, keratin) was neglected in calculations.

The melanin concentration was determined by minimising the goal function

$$F(C_m, \varphi_{eu}) = (\mu_a^{460} - \mu_a^B)^2 + (\mu_a^{540} - \mu_a^G)^2$$

$$+ (\mu_a^{600} - \mu_a^R)^2 \qquad (5)$$

with respect to unknown values of C_m and φ_{eu}. Here, μ_a^{460}, μ_a^{540} and μ_a^{600} are the hair absorption coefficients calculated at wavelengths 460, 540 and 600 nm from the system of equations (4), and μ_a^R, μ_a^G and μ_a^B are the absorption coefficients measured in the spectral regions corresponding to the RGB components of the hair image. Minimisation was performed by the simplex Nelder–Meed method [39]. Iterations were performed until the agreement between theoretical and experimental absorption coefficients within 5%.

The melanin content was additionally controlled by acid-alkali extraction of melanin from black hairs by the method described in [18]. Black hair samples, each weighing 20 g, were completely dissolved in a highly concentrated NaOH alkali solution for three days at a temperature of 4 °C. Then, the solution was neutralised by hydrochloric acid for a day, and the obtained residue was centrifuged (5000 rpm) for 10 min. The residue was washed three times with distilled water during centrifuging (5000 rpm) for 10 min and dried. Depending on the hair sample, the melanin yield was 116–232 mg, corresponding to the concentration range from 5.8 to 11.6 mg g^{-1}. The average melanin concentration was 8.7 ± 4.1 mg g^{-1}.

4. Results and discussion

Table 2 presents diameters and transmission and reflection coefficients for hairs of different types, measured by the method described in section 3. The results of measurements are divided into series (see section 3) and spectral regions corresponding to the colour RGB components. All the data are averaged over 30 hair samples obtained from each of the volunteers, and the root-mean-square deviation is presented for each average value. One can see from Table 2 that hairs of young people are thicker that those of the elders. Note also that dark hairs are thicker than light ones for the same age group.

Analysis of the reflection and transmission coefficients for hairs of different types shows that the reflection coefficient increases, while the transmission coefficient decreases on passing from the blue to red region, which suggests that the scattering coefficients decreases on passing from the short-wavelength to long-wavelength spectral region.

Table 3 presents the values of μ_a and μ_s' calculated from the measured reflection and transmission coefficients by using the inverse Monte-Carlo methods in spectral regions corresponding to the three colour components. One can see from the table that maximum absorption is observed for dark hairs, i.e. for chestnut, black, and dark light brown hairs.

The absorption coefficient of grey hairs is comparatively small, especially in the red region. The absorption coeffi-

Table 3. Optical parameters of hairs of different types obtained by the Monte-Carlo method.

Series number	Red component		Green component		Blue component	
	μ_a/cm^{-1}	μ_s'/cm^{-1}	μ_a/cm^{-1}	μ_s'/cm^{-1}	μ_a/cm^{-1}	μ_s'/cm^{-1}
I	14.5 ± 3.8	40.6 ± 17.4	19.7 ± 5.7	55.8 ± 29.1	34.8 ± 8.9	90.5 ± 48.3
II	28.5 ± 6.3	37.5 ± 18.8	38.6 ± 7.7	53.4 ± 35.6	68.3 ± 8.9	91.3 ± 91.3
III	1.68 ± 0.20	164.5 ± 54.8	3.05 ± 0.53	202.6 ± 92.1	6.4 ± 0.4	278.2 ± 126.5
IV	1.7 ± 0.7	161.1 ± 40.3	3.16 ± 0.12	172.2 ± 42.5	6.8 ± 0.3	229.1 ± 91.6
V	0.9 ± 0.1	175.4 ± 31.8	1.61 ± 0.15	200.7 ± 40.2	3.3 ± 0.4	246.2 ± 63.7
VI	0.75 ± 0.11	182.5 ± 61.1	1.07 ± 0.13	209.4 ± 72.5	1.68 ± 0.25	257.5 ± 102.8
VII	10.3 ± 1.1	78.4 ± 26.5	13.9 ± 2.3	102.8 ± 61.2	24.5 ± 2.9	155.2 ± 124.1
VIII	16.8 ± 4.2	99.4 ± 28.4	22.7 ± 5.5	132.1 ± 80.9	40.1 ± 7.8	203.1 ± 10.7
IX	0.36 ± 0.05	233.6 ± 63.6	0.68 ± 0.11	268.3 ± 83.1	1.4 ± 0.2	331.4 ± 118.2
X	8.71 ± 0.64	105.9 ± 45.1	11.9 ± 0.6	142.3 ± 71.3	20.9 ± 1.3	223.2 ± 167.3

cients of greying and blond hairs have intermediated values. Such a spread in absorption is explained by the structure and morphology of hairs. Dark hairs of young people contain a great amount of melanin, which mainly determines the hair absorption coefficient. By the old age melanosomes in hairs are destructed and no melanin is produced, and we see that for this reason the hairs of a 70 years old brown-haired woman turned grey have much lower absorption coefficient than the hairs of a 19 years old brown-haired girl. The absorption coefficient of hairs of a blond girl is comparable with that of hairs of a 45 years old greying man. The absorption spectra of hairs of all types well agree with the absorption spectrum of melanin, confirming the fact that the absorption properties of hairs are determined first of all by their natural pigment – melanin.

Table 3 also shows that strongest scattering is observed in grey hairs, which is explained by their structural and morphological properties, namely, by a greater roughness of their surface, the presence of voids in hairs, etc. Scattering of light in dark hairs is much weaker, which is obviously related to the size of scatterers in hairs of this type and their denser packing. Finally, the scattering properties of light brown hairs are intermediate between those of dark hairs (brown-haired and blond girls) and grey hairs. It is interesting that the scattering properties of blond hairs are similar to those of greying light-brown hairs, which suggests that hairs of this type have similar structural and morphological properties.

The spectral dependence of the transport scattering coefficient for most of the biological tissues is well approximated by a power function of the type $\mu_s'(\lambda) = a\lambda^{-w}$, where the parameter a is determined by the concentration of scattering centres of the biological tissue and the ratio of the refractive indices of scatterers and the surrounding medium, and the parameter w (wave exponent) characterises the average size of scatterers and determines the spectral dependence of the transport scattering coefficient [3, 42, 43]. The parameter w, as a rule, takes values from 1 to 4. The value $w = 4$ corresponds to shallow, so-called Rayleigh scatterers; in our case, separate keratin fibres of the hair follicle can play the role of such scatterers. The value $w = 1$ corresponds to large, so-called Mie scatterers such as air bubbles in grey hairs. Table 4 presents the results of approximation of the spectral dependences of the transport scattering coefficient given in Table 3 by the above power function.

One can see from Table 4 that the wave exponent for dark and light-brown hairs of young people is ~ 3; this indicates that small scatterers, such as keratin fibres, their bundles, and melanin granules, are dominant in them. In addition, a large content of melanin in hairs of this type (i.e. a large enough number of melanin granules) suggests that melanin granules (at least, in samples studied) have sub-micron dimensions. On the contrary, the parameter w for grey and blond hairs is close to unity. This means that in hairs of this type, the large enough scatters dominate such as surface scales and voids inside hairs. Note the wave exponent for greying hairs has the value equal to ~ 2, which is intermediate between its values for grey and non-grey hairs. This confirms the conclusion made above that the main scatterers in hairs of young people are melanin granules, while scattering in grey hairs is determined by voids inside them.

Table 4. Spectral dependence of the transport scattering coefficient.

Series number	Expression approximating the spectral dependence of the transport scattering coefficient
I	$\mu_s' \approx 9.599 \times 10^9 / \lambda^{3.014}$
II	$\mu_s' \approx 8.181 \times 10^{10} / \lambda^{3.362}$
III	$\mu_s' \approx 5.112 \times 10^7 / \lambda^{1.977}$
IV	$\mu_s' \approx 7.402 \times 10^5 / \lambda^{1.318}$
V	$\mu_s' \approx 6.383 \times 10^5 / \lambda^{1.282}$
VI	$\mu_s' \approx 7.687 \times 10^5 / \lambda^{1.305}$
VII	$\mu_s' \approx 1.043 \times 10^9 / \lambda^{2.564}$
VIII	$\mu_s' \approx 3.102 \times 10^9 / \lambda^{2.698}$
IX	$\mu_s' \approx 1.058 \times 10^6 / \lambda^{1.316}$
X	$\mu_s' \approx 6.487 \times 10^9 / \lambda^{2.803}$

The numerator of approximating expressions presented in Table 4 characterises first of all the number of scattering particles in hairs of different types. One can see from Table 4 that the number of scatterers in hairs of young volunteers is rather high, of the order of 10^9, irrespective of the hair type (dark or light), whereas this number in grey and blond hairs is approximately four orders of magnitude lower ($\sim 10^5$), in good agreement with our scheme of light scattering, i.e. hairs of young people (with a great amount of melanin) contain many quite small and tightly packed scatterers, while the number of scatterers in grey hairs is much smaller but their size is much larger and they are less tightly packed.

The melanin concentration in hairs of different types was determined by minimising the goal function (5) by the method described in section 3 using absorption coefficients obtained by the inverse Monte-Carlo method (Table 3). The results presented in Table 5 show that dark hairs contain the maximum amount of melanin, whereas the melanin concentration in grey and blond hairs is negligibly small. To compare these results with the data reported in the literature (Table 1), the melanin concentration expressed in mg mL^{-1} was recalculated to mg g^{-1} by using the hair density equal to 1.3 g cm^{-3} [44]. The values found in our measurements are in good agreement both with the data from the literature and the results of acid-alkali extraction of melanin from black hairs. Thus, the melanin concentration in black hairs measured by the colour analysis was 9.19 ± 0.38 mg g^{-1}, while this concentration determined by chemical extraction was 8.7 ± 4.1 mg g^{-1}.

The spread of the melanin concentration in black hairs reported in the literature is from 5.37 mg g^{-1} [17] to 31 ± 14.7 mg g^{-1} [18]. We found that blond hairs contain 1.17 ± 0.31 mg g^{-1} of melanin, which well agrees with the melanin concentration 1.1657 mg g^{-1} obtained in [17]. The melanin concentration in chestnut and dark light brown hairs measured in our experiments lies between 2.81 ± 0.11 mg g^{-1} (X series) to 5.38 ± 0.52 mg g^{-1} (VIII series). The spread of the melanin concentration from 1.605 mg g^{-1} [17] to 5.55 mg g^{-1} [12] reported in the literature is also in good agreement with our data. Unfortunately, we failed to find the data on melanin content in grey and greying hairs in the literature; however, melanin concentrations obtained in our experiments well agree with optical, structural and morphological properties of hairs of different types. Note at the same time that we used the averaged value of hair density

Table 5. Melanin concentration in hairs of different types.

Series number	Hair colour	Melanin concentration/mg mL^{-1}	Melanin concentration/mg g^{-1}	Eumelanin concentration/mg mL^{-1}	Pheomelanin concentration/mg mL^{-1}
I	Chestnut	3.61 ± 0.50	4.68 ± 0.65	2.93	0.68
II	Black	7.07 ± 0.29	9.19 ± 0.38	5.74	1.33
III	Light brown with grey hair	0.82 ± 0.37	1.07 ± 0.41	0.11	0.71
IV	White	0.89 ± 0.22	1.17 ± 0.31	0.05	0.84
V	Grey	0.43 ± 0.03	0.56 ± 0.04	0.06	0.37
VI	Grey	0.16 ± 0.02	0.21 ± 0.02	0.14	0.02
VII	Dark light brown	2.52 ± 0.45	3.28 ± 0.51	2.09	0.43
VIII	Dark light brown	4.14 ± 0.83	5.38 ± 0.52	3.41	0.73
IX	Grey	0.20 ± 0.02	0.26 ± 0.02	0.02	0.18
X	Dark light brown	2.16 ± 0.81	2.81 ± 0.11	1.77	0.39

(1.3 g cm^{-3}), whereas the real density can considerably depend on the hair colour and type. It should be expected that dark hairs of young people will have a higher density than grey hairs, which inevitably changes the estimate of the melanin concentration.

Because the question about the melanin type determining the colour and optical parameters of hairs of different types remains open, we estimated the concentrations of eumelanin and pheomelanin for hairs of each type. The results are presented in the last two columns of Table 5. Concentrations of eumelanin and pheomelanin were determined from expressions $C_{eu} = \varphi_{eu} C_m$ and $C_{pheo} = (1 - \varphi_{eu}) C_m$, respectively, by the method described in section 3. One can see from the data presented in Table 5 that eumelanin dominates in dark hairs, whereas pheomelanin dominates in light hairs, in accordance with data obtained in [8–10, 12, 17]. Note, however, that the consideration of absorption of light in other structural components of hairs, for example, keratin, which we neglected in our calculations, can change somewhat the estimates of the total melanin concentration and the ratio of the eumelanin and pheomelanin concentrations.

5. Conclusions

We have developed the experimental setup based on the digital image analysis and estimated by the inverse Monte-Carlo method the optical properties of hairs of different types in three spectral regions corresponding to three colour components. The use of the inverse Monte-Carlo method allowed us to separate for the first time the scattering and absorption properties of hairs. The spectral dependence of light scattering in hairs obtained in our study well agrees with the structural and morphological properties of hairs of different types. The melanin content in hairs of different types has been estimated from their absorption properties. It has been shown that eumelanin dominates in dark hairs, whereas pheomelanin – in light hairs.

At the same time, the optical parameters obtained in our study should be compared with the results of standard spectrophotometric measurements and used for the rigorous solution of the inverse optical problem.

References

1. Tuchin V.V. *Lazery i volokonnaya optika v biomeditsinskikh issledovaniyakh* (Lasers and Fibre Optics in Biomedical Investigations) (Saratov: Saratov State University, 1998).
2. Tuchin V.V. *Tissue Optics: Light Scattering Methods and Instruments for Medical Diagnosis* (Bellingham: SPIE Press, 2000) Vol. TT38.
3. Lopatin V.N., Priezzhev A.V., Aponasenko A.D., Shepelevich N.V., Lopatin V.V., Pozhilenkova P.V., Prostakova I.V. *Metody svetorasseyaniya v analize dispersnykh biologicheskikh sred* (Light Scattering Methods in Analysis of Dispersion Biological Media) (Moscow: Fizmatlit, 2004).
4. Haywood R.M., Linge C. *Lasers Surg. Med.*, **35**, 77 (2004).
5. Hennessy A., Oh C., Diffey B., Wakamatsu K., Ito S., Rees J. *Pigment Cell Res.*, **18**, 220 (2005).
6. Kollias N. *Clinics in Dermatology*, **13**, 361 (1995).
7. Nicholls E.M. *Ann. Hum. Genet. Lond.*, **32**, 15 (1968).
8. Ito S., Jimbow K. *J. Invest. Dermatol.*, **80**, 268 (1983).
9. Menon I.A., Persad S., Haberman H.F., Kurian C.J. *J. Invest. Dermatol.*, **80**, 202 (1983).
10. Thody A.J., Higgins E.M., Wakamatsu K., Ito S., Burchill S.A., Marks J.M. *J. Invest. Dermatol.*, **97**, 340 (1991).
11. Wang X.J., Milner T.E., Dhond R.P., Sorin W.V., Newton S.A., Nelson J.S. *Opt. Lett.*, **20**, 524 (1995).
12. Napolitano A., Vincensi M.R., Donato P.D., Monfrecola G., Prota G. *J. Invest. Dermatol.*, **114**, 1141 (2000).
13. Bashkatov A.N., Sinichkin Yu.P., Genina E.A., Tuchin V.V., Altshuler G.B. *Proc. SPIE Int. Soc. Opt. Eng.*, **4244**, 161 (2001).
14. Zimnyakov D.A., Simonenko G.V., Bashkatov A.N., Genina E.A., Lakodina N.A., Tuchin V.V., Altshuler G.B. *Proc. SPIE Int. Soc. Opt. Eng.*, **4244**, 156 (2001).
15. Zimnyakov D.A., Simonenko G.V., Bashkatov A.N., Genina E.A., Lakodina N.A., Tuchin V.V., Altshuler G.B. *Prib. Tekh. Eksp.*, **5**, 154 (2001).
16. Borges C.R., Roberts J.C., Wilkins D.G., Rollins D.E. *Anal. Biochemistry*, **290**, 116 (2001).
17. Ito S., Wakamatsu K. *Pigment Cell Res.*, **16**, 523 (2003).
18. Liu Y., Kempf V.R., Nofsinger J.B., Weinert E.E., Rudnicki M., Wakamatsu K., Ito S., Simon J.D. *Pigment Cell Res.*, **16**, 355 (2003).
19. Zoccola M., Mossotti R., Innocenti R., Loria D.I., Rosso S., Zanetti R. *Pigment Cell Res.*, **17**, 379 (2004).
20. Andreassi L., Flori L. *Clinics in Dermatology*, **13**, 369 (1995).
21. Barel A.O., Clarys P., Alewaeters K., Duez C., Hubinon J.-L., Mommaerts M. *Skin Res. Technol.*, **7**, 24 (2001).
22. Clarys P., Alewaeters K., Lambrecht R., Barel A.O. *Skin Res. Technol.*, **6**, 230 (2000).
23. Dolotov L.E., Sinichkin Yu.P., Tuchin V.V., Utz S.R., Altshuler G.B., Yaroslavsky I.V. *Lasers Surg. Med.*, **34**, 127 (2004).
24. Hata J., Shimada M., Yamada Y., Uchida A., Itoh M., Nakayama Y., Yatagai T. *J. Biomed. Opt.*, **8**, 93 (2003).
25. Hermanns J.F., Pierard-Franchimont C., Pierard G.E. *Int. J. Cosm. Sci.*, **22**, 67 (2000).

26. Jung B., Choi B., Durkin A.J., Kelly K.M., Nelson J.S. *Lasers Surg. Med.*, **34**, 174 (2004).
27. Kim C.-S., Kim M.K., Jung B., Choi B., Verkruysse W., Jeong M.Y., Nelson J.S. *Lasers Surg. Med.*, **37**, 138 (2005).
28. Rubegni P., Cevenini G., Stanghellini E., Andreassi M., Sbano P., Fabiani P., Andreassi L. *Int. J. Cosmetic Sci.*, **24**, 187 (2002).
29. Stamatas G.N., Kollias N. *J. Biomed. Opt.*, **9**, 315 (2004).
30. Vertuani S., Ziosi P., Solaroli N., Buzzoni V., Carli M., Lucchi E., Valgimigli L., Baratto G., Manfredini S. *Skin Res. Technol.*, **9**, 245 (2003).
31. Kenet R.D. *Clinics in Dermatology*, **13**, 381 (1995).
32. Jones L.N. *Clinics in Dermatology*, **19**, 95 (2001).
33. Nogueira A.C.S., Joekes I. *J. Photochem. Photobiol. B*, **74**, 109 (2004).
34. Rook A., Dowber R. *Bolezni volos i volosistoi chasti golovy* (Diseases of Hairs and Hairy Part of a Head) (Moscow: Meditsina, 1985).
35. Meglinsky I.V., Matcher S.J. *Monte Carlo Methods and Appl.*, **6**, 15 (2000).
36. Meglinski I.V. *Kvantovaya Elektron.*, **31**, 1101 (2001) [*Quantum Electron.*, **31**, 1101 (2001)].
37. Jacques S.L., Wang L. *Optical-Thermal Response of Laser-Irradiated Tissue*. Ed. by A.J. Welch, M.J.C. van Gemert (New York: Plenum Press, 1995) p. 73.
38. Chan D., Schulz B., Rubhausen M., Wessel S., Wepf R. *J. Biomed. Opt.*, **11**, 014029 (2006).
39. Banday B.D. *Basic Optimisation Methods* (London: Edward Arnold, 1984; Moscow: Radio i svyaz', 1988).
40. Prahl S.A., van Gemert M.J.C., Welch A.J. *Appl. Opt.*, **32**, 559 (1993).
41. Jacques S. http://omlc.ogi.edu/spectra/melanin/index.html.
42. Mourant J.R., Fuselier T., Boyer J., Johnson T.M., Bigio I.J. *Appl. Opt.*, **36**, 949 (1997).
43. Schmitt J.M., Kumar G. *Appl. Opt.*, **37**, 2788 (1998).
44. Chernova O.F. http:/bio.1september.ru/article.php?ID=200301501.